Published in final edited form as:
Cell Rep. 2014 October 23; 9(2): 605–617. doi:10.1016/j.celrep.2014.09.004.

An MHC Class II Dependent Activation Loop Between Adipose Tissue Macrophages and CD4+ T cells Controls Obesity-Induced Inflammation

Kae Won Cho[1,6], **David L. Morris**[1], **Jennifer L. DelProposto**[1], **Lynn Geletka**[1], **Brian Zamarron**[2], **Gabriel Martinez-Santibanez**[1], **Kevin A. Meyer**[3], **Kanakadurga Singer**[1], **Robert W. O'Rourke**[3,4], and **Carey N. Lumeng**[1,2,5]

[1]Department of Pediatrics and Communicable Diseases, University of Michigan Medical School, Ann Arbor, MI, 48109. USA

[2]Graduate Program in Immunology, University of Michigan Medical School, Ann Arbor, MI, 48109. USA

[3]Department of Surgery, University of Michigan Medical School, Ann Arbor, MI, 48109. USA

[4]Department of Surgery, Ann Arbor Veteran's Administration Hospital, Ann Arbor, MI, 48109. USA

[5]Department of Molecular and Integrative Physiology, University of Michigan Medical School, Ann Arbor, MI, 48109. USA

[6]Soonchunhyang Institute of Medi-bio Science, Soonchunhyang University, Cheonan-si, Chungcheongnam-do, Korea

Summary

An adaptive immune response triggered by obesity is characterized by the activation of adipose tissue $CD4^+$ T cells by unclear mechanisms. We have examined if interactions between adipose tissue macrophages (ATMs) and $CD4^+$ T cells contribute to adipose tissue metainflammation. Intravital microscopy identifies dynamic antigen dependent interactions between ATMs and T cells in visceral fat. Mice deficient in major histocompatibility complex class II (MHCII) showed protection from diet-induced obesity. Deletion of MHCII expression in macrophages led to an adipose tissue specific decrease in the effector/memory $CD4^+$ T cells, attenuation of $CD11c^+$

Contact: Carey Lumeng M.D. Ph.D. University of Michigan Medical School, 2057 Biomedical Sciences Research Building, 109 Zina Pitcher Place, Ann Arbor, MI 48109-2200, Phone: (734) 615-6242, clumeng@umich.edu

Author Contributions: K.W.C, D.L.M., J.L.B., K.S., L.G., B.Z., G.M-S., and C.N.L. performed, designed, and interpreted the experiments performed. K.A.M. and R.W.O. contributed to human sample collection and analysis. K.W.C. and C.N.L prepared the manuscript. All authors approved the final manuscript.

The authors have no conflicts of interest.

Supplemental Information: Supplemental Figures S1-S6.
Supplemental Movies S1 and S2.

ATM accumulation, and improvement in glucose intolerance by increasing adipose tissue insulin sensitivity. Ablation experiments demonstrated that the maintenance of proliferating conventional T cells is dependent on signals from $CD11c^+$ ATMs in obese mice. These studies demonstrate the importance of MHC Class II restricted signals from ATMs that regulate adipose tissue T cell maturation and metainflammation.

Introduction

Obesity-induced adipose tissue inflammation is controlled by a diverse network of leukocytes comprised of multiple cellular regulators of innate and adaptive immunity (Mathis, 2013). One component of the metainflammatory response to obesity is an alteration in the state of adipose tissue T cells (ATTs) that influences the inflammatory set point of adipose tissue and insulin sensitivity. Adipose tissue contains a unique population of resident regulatory T cells (Treg) that are prominent in lean states and have a protective influence on adipose tissue inflammation in obesity (Cipolletta et al., 2012; Deiuliis et al., 2011; Feuerer et al., 2009). While Tregs are down regulated with obesity, conventional Th1 T cells (Tconv) accumulate in visceral fat depots and contribute to pro-inflammatory signals in adipose tissue (Khan et al., 2014; Stolarczyk et al., 2013; Winer et al., 2009). The ability of Th1 ATT cells to promote obesity-induced inflammation is dependent on αβ T-cell receptors, T-bet, STAT3, and IFNγ (Khan et al., 2014; O'Rourke et al., 2012; Priceman et al., 2013; Rocha et al., 2008; Stolarczyk et al., 2013). Th17 and Th22 cells in adipose tissue have also been associated with insulin resistance in obese individuals (Bertola et al., 2012; Fabbrini et al., 2013).

The signals that control the activation and maintenance of the adipose tissue T cells are not well understood. Obesity induces ATT cell proliferation suggesting that ATT cells are stimulated by signals from the adipose tissue environment (Moraes-Vieira et al., 2014; Morris et al., 2013). Both Treg and Tconv have a limited repertoire of T cell receptors suggesting that clonal T cell selection shapes adipose tissue lymphocytes (Feuerer et al., 2009; Yang et al., 2010). Compared to secondary lymphoid tissues, adipose tissue contains few naïve T cells and a high percentage of effector/memory type $CD4^+$ T cells which regulate adaptive immunity based on interactions with antigen presenting cells (APCs) (Reis e Sousa, 2006; Vandanmagsar et al., 2011; Yang et al., 2010; Zhu and Paul, 2008). APCs integrate multiple signaling pathways in tissues resulting in the maturation of naïve T cells towards a specific activation profile. For $CD4^+$ T cells, a core component of the maturation process is the presentation of antigens via major histocompatibility complex II (MHCII) which bind to the T cell receptor.

Several lines of evidence suggest that APCs partner with T cells in adipose tissue to control metainflammation. Global deficiency of MHCII protects mice from obesity-induced obesity and inflammation (Deng et al., 2013). Conversely, enhancing APC function in fat by injection of activated bone marrow derived dendritic cells into mice promotes adipose tissue inflammation and induces insulin resistance (Moraes-Vieira et al., 2014; Stefanovic-Racic et al., 2012). Adipokines such as leptin, adiponectin, and RBP4 activate APCs and promote Th1 T cell activation (Jung et al., 2012; Mattioli et al., 2005; Moraes-Vieira et al., 2014).

APC signals also play a role in the maintenance of protective adipose tissue Tregs. B7 deficient mice that lack co-stimulatory molecules CD80 and CD86 have reduced Tregs systemically and in adipose tissue and demonstrate worse adipose tissue inflammation (Zhong et al., 2014).

While APCs may shape ATTs, ATTs can also influence the recruitment and activation of adipose tissue macrophages (ATMs). ATT activation precedes the prominent accumulation of pro-inflammatory $CD11c^+$ ATMs induced by chronic obesity (Nishimura et al., 2009; Winer et al., 2009). This observation implies that the machinery required to activate ATT cells in response to obesity must be native to adipose tissue and exist prior to the onset of obesity. In all adipose depots in lean mice and humans, the most prominent professional APCs are the extensive network of $MHCII^+$ resident ATMs (Lumeng et al., 2007; Odegaard and Chawla, 2011). Resident ATMs express markers of alternatively activated macrophages (CD206 and CD301/MGL1), do not express the activation marker CD11c ($CD11c^-$), and are concentrated in fat associated lymphoid clusters (FALCs) and omental milky spots (Morris et al., 2013; Rangel-Moreno et al., 2009).

Work from our group and others have shown that ATMs are functional APCs that can promote antigen specific T cell activation *ex vivo* and in adipose tissue (Bertola et al., 2012; Morris et al., 2013; Stefanovic-Racic et al., 2012). However, several unresolved questions remain regarding if MHC Class II restricted signals from ATMs are required for the activation of $CD4^+$ T cells in adipose tissue, the importance of MHCII signals in insulin resistance, and which subtype of ATM (resident or recruited $CD11c^+$) are required for initiating an adaptive immune response to obesity. The goal of this study was to investigate the role that ATMs play in directing $CD4^+$ ATT cell activation, adipose tissue inflammation, and insulin resistance *in vivo*. We reveal a dynamic and antigen dependent network of immune surveillance driven by interactions between ATMs and ATT cells in visceral adipose tissue *in vivo*. Interruption of communication between resident tissue ATMs and ATTs via macrophage specific deletion of MHCII does not alter adipose tissue T cells in lean states, but prevents the generation of effector/memory ATT cells and adipose tissue insulin resistance with obesity. Ablation of $CD11c^+$ cells in obese mice support the importance of $CD11c^+$ ATMs in maintaining Tconv at the expense of Treg. Overall, our studies identify a critical MHCII-restricted activation loop between resident $CD11c^-$ ATMs, ATTs, and $CD11c^+$ ATMs that contributes to metainflammation.

Results

$CD4^+$ T Cells Demonstrate Antigen-Dependent Interactions With Adipose Tissue Macrophages (ATMs) *In Vivo*

We have previously identified high concentrations of $CD4^+$ ATTs in FALC structures in visceral adipose tissue that are also enriched for $MHCII^+$ $CX3CR1^+$ ATMs (Morris et al., 2013). To better delineate relationship between $CD4^+$ T cells and ATMs in FALCs, we performed confocal microscopy on whole mount adipose tissue samples. FALCs contained $Mgl1^+$ ATMs that co-expressed MHCII (Figure 1A). MHCII was not identified in $caveolin^+$ adipocytes in lean or high fat diet (HFD) fed obese mice. Imaging of human omental adipose tissue from obese patients undergoing bariatric surgery identified milky spots

enriched for $CD206^+$ $HLA\text{-}DR^+$ ATMs (Figure 1B). $HLA\text{-}DR^+$ cells were in direct contact with $HLA\text{-}DR^-$ $CD4^+$ T cells in milky spots. As in mice, no HLA-DR staining was observed in association with adipocytes.

We employed live intravital microscopy to evaluate the dynamic interactions between ATMs and $CD4^+$ ATT cells *in vivo*. CFSE-labeled $CD4^+$ T cells from OT-II mice were injected IP into CD11c-mCherry reporter mice that permitted identification of endogenous myeloid cells (Khanna et al., 2010). Flow cytometry demonstrated that the $mCherry^+$ cells were $F4/80^+$ $CD11b^+$ ATMs in lean mice (Figure S1A). 24 hours after injection, recipient mice were anesthetized and epididymal white adipose tissue (eWAT) was externalized for imaging. More than 20% $CD4^+$ T cells isolated from eWAT were $CFSE^+$ (∼15% of injected cells were recovered in adipose tissue) and concentrated in FALC structures (Figure 1C and S1B-C). Cells were imaged by multiphoton confocal microscopy for 20 minutes. While $mCherry^+$ cells did not demonstrate significant motility, the $CD4^+$ T cells were highly motile (mean velocity = 5.6 μm/min) and showed random movement within the FALC structure (Figure 1D-E, Movie S1).

The interactions between $CD4^+$ T cells and APCs are increased in the presence of a cognate T cell specific antigen (Halin et al., 2005; Koltsova et al., 2012). To examine this in adipose tissue, CD11c-mCherry mice were injected IP with CFSE-labeled $CD4^+$ OT-II T cells followed by injection of ovalbumin (OVA) or BSA control. After 2 hours, $CD4^+$ T cell velocity and path of movement were assessed with intravital microscopy (Figure 1F-G). In BSA-injected mice, velocity of $CD4^+$ T cells and displacement length were 5.53 ± 0.36 μm/min and 25.14 ± 0.52 μm respectively over 20 minutes. In control mice, less than 20% of the T cells directly interacted with $mCherry^+$ cells based on colocalization (Figure 1H). Among the motile $CD4^+$ cells, ∼2% of the cells showed distinct high velocity motile behavior. With OVA injection, long-lived T cell-$CD11c^+$ cells interactions were induced and ∼60% of the CD4+ T cells maintained stable contact with the $mCherry^+$ cells over 20 minutes (Figure 1H and Movie S2). With OVA, the average speed (2.2 ± 0.14 μm/min) and mean displacement length (BSA vs OVA: 25.15 ± 0.52 μm vs 14.73 ± 1.2 μm; $p<0.05$) of $CD4^+$ T cells were decreased compared to controls. The reduction in migration velocity with OVA was due to a reduction in mean individual T cell motility as well as the loss of the high motility T cells seen in control mice. In sum, intravital imaging demonstrates that dynamic interactions between ATMs and $CD4^+$ T cells in adipose tissue are constantly occurring in adipose tissue and such interactions are stabilized and enhanced in an antigen-dependent manner.

MHCII Is Required for HFD-Induced Adipose Tissue Inflammation and Insulin Resistance

Since MHCII is required for cell-mediated immunity through $CD4^+$ T cells, we examined the requirement for MHCII in the generation of obesity-induced inflammation by studying MHCII deficient mice (*H2-Ab1*$^{-/-}$, MHCIIKO). Lean MHCIIKO mice weighed less then age-matched wild type (WT) mice and gained less weight with age (Figure 2A). When challenged with HFD for 20 weeks, MHCIIKO mice gained weight at a reduced rate compared to WT controls (WT 27.8 ± 0.6g; MHCIIKO 20.6 ± 1.2g; $p<0.01$). Metabolic cage analysis did not identify any differences in food intake, energy expenditure, or body

length between genotypes in either diet condition (Figure S2). Body composition analysis showed that the weight differences between genotypes were due to a decrease in lean body mass, but not fat mass, in ND and HFD MHCIIKO mice (Figure 2B). When body composition was expressed as a percentage of total body mass, there were no differences between genotypes in ND and HFD conditions. Tissue weights at sacrifice demonstrated significantly more visceral adiposity in HFD fed MHCIIKO compared to WT (Figure 2C). HFD fed WT and MHCIIKO mice demonstrated similar hypertrophy of inguinal/subcutaneous fat depots (sWAT). HFD fed mice demonstrated significant accumulation of $Mac2^+$ crown-like structures (CLS) in WT eWAT while CLS were largely absent in MHCIIKO adipose tissue consistent with a preservation of adipose tissue health and low inflammation (Figure 2D). Adipocyte size did not differ between HFD fed WT and MHCIIKO mice. (Figure 2E). Liver weights of MHCIIKO mice were significantly less than WT mice in both dietary conditions and HFD did not induce an increase in liver weight in MHCIIKO mice (Figure 2C). HFD MHCIIKO mice were protected from histologic steatosis and liver triglyceride accumulation (Figure S3A). This protection was associated with a significant decrease in hepatic *Scd1* and *Fasn* expression in MHCIIKO mice (Figure S3D).

Glucose and insulin tolerance were not altered in ND fed MHCIIKO mice (Figure 2F-G). Despite an increase in visceral adipose tissue, obese MHCIIKO mice had improved glucose and insulin tolerance compared to HFD WT mice. Insulin levels and free fatty acids were significantly lower in obese MHCIIKO mice compared to WT (Figure S3B). Gene expression analysis of eWAT from HFD mice showed increased expression of genes associated with adipocyte insulin sensitivity (e.g. *Glut4, Pparγ,* and *Adipoq* in MHCIIKO mice compared to WT (Figure S3C). In addition, MHCIIKO mice showed decreased expression of *Ifng* in eWAT, indicating that MHCII-restricted signals are required for maximal *Ifng* induction with obesity. In liver, there were no significant differences in *Ifng, Tnfa, Il6,* or *Foxp3* gene expression between WT and MHCIIKO mice in response to HFD (Figure S3D). Overall, these data demonstrate that MHCII dependent signals contribute to insulin resistance with diet-induced obesity by promoting adipose tissue dysfunction and hepatic lipid accumulation.

MHCII Deficiency Reduces the Accumulation of $CD11c^+$ ATMs and $CD4^+$ ATTs but Not CD8+ ATTs in Response to HFD

To examine the effects of MHCII on leukocyte infiltration into visceral fat, ATM and ATT content was assessed by flow cytometry in eWAT from WT or MHCIIKO mice. Consistent with the imaging data, MHCIIKO mice had fewer ATMs due to a decrease in the percentage of $CD11c^+$ ATMs (Figure 2H). The reduction in $CD11c^+$ ATM accumulation could not be explained by reduced MCP-1 or reduced circulating monocyte levels, as *Ccl2* expression in eWAT and the content of $7/4^{hi}$ blood monocytes were similar between HFD fed WT and MHCIIKO mice (Figure S3C and S3E). Consistent with the importance of MHCII in thymic selection of $CD4^+$ T cells, MHCIIKO mice had a significant reduction in $CD4^+$ lymphocytes in the blood, spleen, and adipose tissue compared to WT mice in both diet conditions (Figure 2I-J, data not shown). A substantial reduction of $CD4^+$ ATT cells as a percent of stromal vascular cells (SVCs) was seen for both Tconv ($CD4^+$ $FoxP3^-$) as well as Tregs ($CD4^+$ $FoxP3^+$). $CD8^+$ T cells were significantly increased systemically and in adipose

tissue of MHCIIKO mice. These results suggest that neither an increase in $CD8^+$ ATTs nor a reduction in Tregs alone is sufficient to generate maximal adipose tissue inflammation and insulin resistance and suggest an important role for MHCII dependent Tconv in obesity-induced inflammation.

Macrophage-Specific MHCII Deficient Mice Show Improved Insulin Sensitivity in Response to HFD

The systemic depletion of $CD4^+$ cells in whole body MHCIIKO mice does not let us discern the role of adipose tissue specific MHCII in regulating T cells. To address this, initial experiments attempted to delete MHCII expression in hematopoietic cells via bone marrow transplantation of $MHCII^{-/-}$ donors into WT recipients. However, similar to other reports (Marguerat et al., 1999), these mice developed an autoimmune phenotype with severe weight loss that limited our ability to assess metabolic responses (Data not shown).

Resident $CD301^+$ ATMs are the dominant professional APC in adipose tissue by quantity in lean states and are thus poised to initiate T cell activation in response to obesogenic signals (Bertola et al., 2012; Stefanovic-Racic et al., 2012). To evaluate the hypothesis that MHCII signals from resident ATMs are required for obesity-induced activation of $CD4^+$ ATT cells, we generated macrophage-specific MHCII knockout (MMKO) mice. LysM-Cre mice were crossed to mice with *flox* sequences flanking exon 1 of the *H2-ab1* gene ($H2\text{-}Ab1^{tm1Koni}$; $MHCII^{f/f}$). Flow cytometry confirmed MHCII expression in both ATMs and ATDCs in $MHCII^{f/f}$ control mice. In this experiment, the macrophage specific marker CD64 was used to identify ATMs (resident $CD45^+$ $CD64^+$ $CD11c^-$ and recruited $CD45^+$ $CD64^+$ $CD11c^+$) and distinguish them from ATDCs ($CD45^+$ $CD64^-$ $CD11c^+$)(Gautier et al., 2012) (Figure 3A). Lean MMKO did not demonstrate any differences in the quantity of ATMs or ATDCs in eWAT compared to controls (Figure 3B). However, MHCII expression was absent in >95% of the ATMs of MMKO mice and remained intact in a small but prominent population of ATDCs. Immunostaining of adipose tissue confirmed deletion of MHCII in $MGL1^+$ resident ATMs in MMKO mice (Figure 3C). Expression of *MHCII (H2-ab1*) in eWAT was decreased by >95% in MMKO mice without changing *Emr1*, *CD40*, or *CD80* expression demonstrating that LysM-cre expressing cells account for the vast majority of *MHCII* expression in adipose tissue (Figure 3D). MMKO mice had normal numbers of circulating neutrophils and monocytes indicating the macrophage MHCII is not required for the proper maintenance of myeloid cells (Figure 3E). Importantly, there were no changes in $CD4^+$ or $CD8^+$ T cells in the thymus, spleen, and lymph nodes of MMKO mice demonstrating that macrophage MHCII is dispensable for normal T cell maturation in lymphoid tissues (Figure 3F).

To determine the importance of macrophage MHCII in glucose metabolism, control and MMKO mice were fed with ND or HFD for 14 weeks. MMKO mice were healthy and demonstrated weight gain with HFD that was identical to control mice (Figure 4A) suggesting that macrophage MHCII does not account for the growth defects observed in whole body MHCIIKO mice. eWAT hypertrophy on HFD was similar between control and MMKO mice (Figure 4B). Fasting glucose and insulin levels did not differ between ND fed control and MMKO mice (Figure 4C). HFD fed MMKO mice showed a significant decrease

in fasting glucose levels compared to control mice although fasting insulin levels were similar. Glucose and insulin tolerance tests did not differ between ND fed control and MMKO mice (Figure 4D-E). However, when challenged with HFD, MMKO mice had significantly improved glucose tolerance and insulin sensitivity compared to controls.

Immunofluorescence microscopy showed a reduction in CLS in eWAT from obese MMKO mice compared to controls without differences in adipocyte size (Figure 4F-G). To evaluate the mechanisms of improved insulin sensitivity in MMKO mice, adipose tissue and liver insulin signal transduction was evaluated in obese mice. Consistent with the decrease in CLS, HFD fed MMKO mice demonstrated a significant increase in Akt phosphorylation in eWAT in response to insulin compared to WT mice (Figure 4H). Insulin-stimulated Akt phosphorylation in the liver was marginally increased in MMKO mice compared to controls (Figure 4I). Gene expression from whole adipose tissue demonstrated a significant increase in adiponectin (*Adipoq*) and *Glut4* expression in EWAT from obese MMKO mice compared to WT (Figure 4J). These observations indicate that MMKO mice are protected from insulin resistance by improvements in adipose tissue insulin sensitivity.

Accumulation of CD11c$^+$ ATMs in Visceral Fat Is Attenuated in MMKO Mice

To examine the cellular mechanisms involved in the improved metabolism of MMKO mice, ATM and ATDC content was analyzed by flow cytometry (Figure 5A). There were no significant differences in total ATMs or ATDCs in eWAT between control and MMKO mice in lean or obese states (Figure 5B). In ND fed mice, the quantity of CD11c$^+$ and CD11c$^-$ resident ATMs as a percentage of SVCs did not differ between genotypes. However, with HFD, obese MMKO mice had significantly fewer CD11c$^+$ ATMs compared to controls. No changes in the quantity of resident CD11c$^-$ ATMs were observed in MMKO mice, resulting in an overall decrease in the ratio of CD11c$^+$ to CD11c$^-$ ATMs in obese MMKO mice (Figure 5C). Consistent with this, the M1 macrophage marker, *Nos2* was decreased in eWAT and the alternatively activated macrophage marker *Arg1* showed a trend towards an increase (Figure 5D). To evaluate if differences in proliferation account for the decrease in CD11c$^+$ ATMs, tissue sections were stained with Ki67. No differences in Ki67$^+$ cells in the ATM enriched CLS were observed (Figure 5E). Analysis of serum from obese mice identified a significant decrease in MCP-1 levels in MMKO mice compared to WT controls (Figure 5F). Bone marrow derived macrophages were generated from WT and MMKO mice and no differences in inflammatory gene expression in response to LPS was observed suggesting that MHCII is not required for macrophage activation (Figure 5G). In agreement with the lower MCP-1 and ATM accumulation, expression of genes associated with inflammation such as *Tnfa* and *Il10* in eWAT and liver from obese MMKO was decreased compared to obese WT controls (Figure S4A-B). Collectively, these results indicate that the presence of MHCII on resident ATMs is required for maximal recruitment of CD11c$^+$ ATMs to visceral adipose tissue, inflammation, and metabolic dysfunction.

The Activation of Conventional CD4$^+$ ATT Is Dependent on Macrophage MHCII

We next examined the effect of MHCII deficiency in resident ATMs on ATT cells. The total amount of CD3$^+$ lymphocytes in eWAT was not significant different between control and MMKO mice on ND or HFD (Figure 6A). While the quantity of CD4$^+$ ATTs was similar

between lean WT and MMKO mice, obese MMKO mice had fewer $CD4^+$ ATTs in eWAT compared to HFD controls (Figure 6B). In ND mice, there were no differences between MMKO and controls in the quantity of Tconv and Treg in eWAT (Gating shown in Figure S5A). However, with HFD Tconv expansion was blocked in MMKO mice (Figure 6C). In our cohorts, Tregs increased with HFD as a percentage of SVCs in control mice, but this was blunted in MMKO mice (Figure S5B). Despite the selective reduction in $CD4^+$ ATT in MMKO mice, no significant differences in proliferating Ki-67^+ $CD4^+$ ATT cells were observed in ND or HFD-fed MMKO mice compared to controls (Figure 6D). Lean MMKO mice demonstrated an increase in the number of $CD8^+$ ATTs in eWAT (Figure 6B). With HFD, $CD8^+$ ATTs increased to a similar degree in control and MMKO mice.

Quantitation of naïve, effector-memory (E/M) and central-memory (C/M) $CD4^+$ T cell subsets demonstrated similar numbers of these subsets in ND fed MMKO and control mice (Figure 6E-G) suggesting that homeostatic ATT cell proliferation is MHCII independent. HFD exposure decreased naïve $CD4^+$ ATTs and increased E/M $CD4^+$ ATTs in eWAT in WT mice. In contrast, HFD-fed MMKO mice retained similar percentages of naïve T cells as ND mice and had a decrease in the number of E/M ATT cells. No significant changes in C/M ATTs were observed between genotypes in either diet condition (data not shown). These changes in $CD4^+$ T cells were adipose tissue specific as no differences in the frequency of $CD4^+$ T cell, $CD8^+$ T cells, Tconv, Treg and proliferation was observed in the spleens of obese control and MMKO mice (Figure S5C). Gene expression analyses identified slight reductions *Il2*, a critical regulator of T cell activation, in eWAT from MMKO mice (Figure S4A). No differences in transcription factors critical for Th1, Th2, and Th17 differentiation (*Tbet, GATA3, RORg*) or polarization signals (*Il4*) were seen in whole eWAT from obese WT and MMKO mice. Gene expression analysis of FACS purified $CD4^+$ T cells from eWAT from MMKO mice showed a significant decrease in *Ifng* expression compared to WT (Figure 6H). This difference was specific to adipose tissue T cells as *Ifng* expression in splenic $CD4^+$ T cells did not differ between MMKO and WT mice (Figure S5C). These findings suggest that the maturation of $CD4^+$ ATTs with chronic HFD is dependent on ATM derived MHCII.

Ablation of $CD11c^+$ Cells Reduces $CD4^+$ ATT Cell Accumulation and Proliferation in Obese Mice

The MMKO results demonstrate the importance of resident $CD11c^-$ ATMs in initiating ATT activation in response to obesity. Since an increase in APC function is associated with the accumulation of $CD11c^+$ ATMs in obese mice, we examined the importance of $CD11c^+$ ATMs in sustaining T cell activation in established obesity using a $CD11c^+$ cell ablation model. Chimeric CD11c-DTR mice were generated by transplanting bone marrow from CD11c-DTR transgenic mice (CD45.2) into lethally irradiated wild-type recipients (CD45.1) (Figure 7A). Six weeks after reconstitution, chimeric mice were fed a ND or HFD for 6 weeks. Mice were then injected IP with PBS or diphtheria toxin (DT) every other day for two weeks while continuing the diets. No significant changes in total body weight or eWAT mass were observed with DT injection (Figure S6A-B). Efficient ablation of $CD11c^+$ ATMs was confirmed by flow cytometry (Figure 7B). As expected, in control mice, HFD increased total eWAT ATM content and induced $MHCII^{high}$ $CD11c^+$ ATMs (Figure 7C-D). DT

injection led to a slight decrease in total ATMs in lean mice and significantly decreased the number of ATMs in HFD mice. CD11c ablation did not alter fasting glucose levels or glucose tolerance in ND fed mice but normalized fasting glucose levels and significantly improved glucose tolerance. (Figure S6C-D).

We next examined the effect of $CD11c^+$ ATM ablation on ATT cells. In PBS controls, the quantity of $CD3^+$ ATT cells in eWAT increased in response to HFD (Figure 7E). Ablation of $CD11c^+$ ATMs did not alter $CD3^+$ ATT cells in ND fed mice, but led to a significant decrease in $CD3^+$ ATT cells in obese mice. This decrease was driven by a decrease in $CD4^+$ T cells (Figure 7F). Depletion of $CD11c^+$ ATMs in HFD mice decreased the number of Tconv, while Tregs increased in eWAT in the DT treated group (Figure 7G). This resulted in a significant decrease in the ratio of Tconv to Tregs induced by with CD11c cell ablation in both diet groups. $CD4^+$ ATT proliferation was assessed by BrDU incorporation. HFD increased the proliferation of Tconv in controls (Figure 7H-J). Ablation of $CD11c^+$ ATMs did not alter Tconv or Treg proliferation in ND mice. However, depletion of $CD11c^+$ ATMs in HFD mice decreased Tconv proliferation and enhanced Treg proliferation in adipose tissue. Gene expression analysis of eWAT showed that depletion of $CD11c^+$ ATMs decreased expression of genes associated with T cell activation (*Il2* and *Il12*) and increased expression of genes associated with Treg function (*Foxp3, GATA3* and *Il10*) (Figure 7K). Overall, these data suggest that $CD11c^+$ ATMs contribute to the maintenance Tconv ATTs at the expense of Tregs in obese mice.

Discussion

Our studies suggest important roles for both resident $CD11c^-$ and recruited $CD11c^+$ ATMs as initiators and effectors of adipose tissue inflammation via their communication with ATTs via MHCII (Figure 7L). Chronic adipose tissue expansion leads to events that compromised adipocyte function (e.g. hypoxia, ER stress). $MHCII^+$ resident ATMs ($CD11c^-$ $MGL1/CD301^+$ in mice) reside in close proximity to adipocytes and sample the environment. ATT cells transit throughout adipose tissue and FALCs/milky spots where they interact transiently with $MHCII^+$ ATMs. Interactions between ATTs and ATMs are enhanced by cognate antigens to potentiate T cell activation and conversion of naïve to effector/memory T cells. MHCII in resident ATMs is required to translate obesogenic cues into a maturation of Tconv to this effector/memory phenotype with increased IFNγ expression. Disruption of class II signals in resident ATMs prevents the downstream accumulation of pro-inflammatory $CD11c^+$ ATMs and preserves adipocyte insulin sensitivity. Once established, $CD11c^+$ ATMs support the continued activation and proliferation of Tconv at the expense of Tregs to promote insulin resistance.

Macrophage MHCII is not required for T cell maturation in primary and secondary lymphoid tissues permitting us to identify adipose tissue specific effects. Deletion of MHCII in macrophages (MMKO mice) does not alter ATT cell development consistent with the MHCII-independent homeostatic proliferation of tissue memory T cells (Surh and Sprent, 2008). However, loss of macrophage class II restricted signals impairs their activation with obesity demonstrating the importance of ongoing T cell education and selection in adipose tissue. This is consistent with the unique profile of adipose tissue Tregs (Feuerer et al.,

2009). Consistent with reports of a role for MHCII in shaping CD8 maturation (Do et al., 2012), both MMKO and MHCIIKO mice have an increase in adipose tissue $CD8^+$ cells suggesting that an increase in $CD8^+$ T cells in fat alone is not sufficient to potentiate insulin resistance. Moreover, MHCIIKO mice have a significant reduction in Tregs, yet are protected from obesity-induced inflammation. This finding seems to be at odds with other studies demonstrating that Tregs are the sole protective factor in adipose tissue that prevents inflammation. Our experience examining adipose tissue Tregs in lean and obese mice has differed from other reports as we do not consistently see a decrease in adipose tissue Tregs with obesity as a percentage of $CD4^+$ T cells. Due to the increase in total $CD4^+$ T cells in the SVF with obesity, we frequently observe an increase in Tregs as a percentage of the SVF consistent with other reports (Deiuliis et al., 2011; Winer et al., 2009). We are unsure of why our results differ from other groups on this point, but differences in animal husbandry conditions may contribute to Treg variation.

Our results with macrophage specific MHCII deletion and ablation of $CD11c^+$ cells are complementary and reveal distinct *in vivo* functions of ATM subtypes in T cell activation. While the MMKO mice argue for a critical role for resident ATMs in the initiation of T cell activation with obesity, CD11c-DTR experiments suggest an important role for CD11c+ ATMs in sustaining this activated state. Similar to other reports, ablation of $CD11c^+$ ATMs in obese animals reverses insulin resistance and adipose tissue inflammation (Patsouris et al., 2008). Our results link these improvements to a decrease in the number and proliferative capacity of Tconv and an increase in Tregs when $CD11c^+$ ATMs are ablated. This demonstrates the importance of both ATM subtypes in regulating T cell activation. Resident ATMs participate in the initiation of inflammatory cascades via MHCII to induce $CD11c^+$ ATMs. However, in an established obese inflammatory environment, $CD11c^+$ ATMs play an important role in sustaining conventional T cell proliferation and suppressing Tregs.

Our data demonstrate a critical role ATMs play in priming $CD4^+$ T cells and sustaining adaptive immune responses to obesity *in vivo* and are consistent with *in vitro* studies (Moraes-Vieira et al., 2014; Morris et al., 2013). Adipocytes have been shown to induce MHCII gene expression with obesity and reactivate antigen primed T cells *in vitro* (Deng et al., 2013). Our studies have found little evidence to support significant MHCII protein expression on adipocytes in obese mice or human adipose tissue samples relative to ATMs. By gene expression, macrophages account for >95% of the MHCII expression in adipose tissue (residual $MHCII^+$ adipose tissue DCs remain in our MMKO mice) arguing that non-macrophage cells such as adipocytes play a minor role in MHCII expression in adipose tissue. Our studies show that $CD4^+$ ATT cells interact with ATM derived MHCII much more frequently in their environment. However, it is clear that regulation of T cell homeostasis is not purely MHCII dependent and it is likely that adipocyte derived signals influence T cell function and activation.

A major unanswered question in the field is the nature of the antigen that is being presented by ATMs and sensed by T cells. We can only speculate on the nature of this signal. The identification of clonal expansion of $CD4^+$ T cells is a feature of atherosclerosis and type 1 diabetes, however the identification of key antigens in these disease settings has also been elusive. Our studies suggest that therapeutic interventions that target APC-T cell

communication may play a role in the treatment of insulin resistance and type 2 diabetes. In mice, MHCII antibody blockade decreased $CD4^+$ ATTs, but did not result in significant improvement in glucose tolerance (Morris et al., 2013). This may be due to improper dosing or window of intervention and will need to be revisited in light of our current work. Nonetheless, our findings suggest an overlap between efforts to block T cell TCR signaling and co-stimulation in autoimmune diseases such as multiple sclerosis and type 1 diabetes and obesity-associated metainflammation (Podojil and Miller, 2009). It also implies that anti-diabetic treatments and therapies targeting adipokines such as RBP4 may play critical roles in modulating APC function of resident and $CD11c^+$ ATMs.

An important implication of our MMKO mouse model is that the ATM may be a unique cells that if targeted can provide beneficial effects in peripheral tissue responses without altering systemic T cells. Macrophages are thought to have less potent APC function than classical DCs. Our data suggest that adipose tissue may be a unique environment dominated by ATMs with strong APC activity that partner with T cells to establish an interaction network that perpetuates metainflammation.

Experimental Procedures

Animals Studies

C57BL/6J, LysMCre (B6.129P2-Lyz2^{tm1cre1fo}/J), MHCII$^{f/f}$ (B6.129X1-H2-Ab1^{tm1Koni}/J), CD11c-DTR (B6.FVB-Tg(Itgax-DTR/EGFP)57Lan/J) and OT-II (B6.Cg-Tg(TcraTcrb)425Cbn/J) mice were purchased from the Jackson Laboratory. MHCIIKO (B6.129-H2-Ab1^{tm1Gru} N12) and wild type (B6.SJL-*Ptprc*^{a}/BoyAiTac) male mice were purchased from Taconic. CD11c-mCherry mice were kindly provided by Dr. Kamal Khanna (University of Connecticut). Macrophage-specific MHCII KO mice (MMKO) were generated by breeding LysM-Cre with MHCII$^{f/f}$ mice. Cre-negative MHCII$^{f/f}$ littermates were used as control. Male mice were *ad libitum* fed a normal diet (4.5% fat; PMI Nutrition International) or fed a HFD consisting of 60% fat (Research Diets) beginning 6 weeks of age. All mice procedures were approved by the University Committee on Use and Care of Animals (UCUCA) at the University of Michigan and were conducted in compliance with the Institute of Laboratory Animal Research Guide for the Care and Use of Laboratory Animals.

Bone marrow transplantation

Bone marrow transplants were performed as described (Singer et al., 2013). Reconstitution was confirmed 6 weeks after transplantation, and recipient animals were fed either normal diet or HFD for 8 weeks. For $CD11c^+$ cell depletion, diphtheria toxin (DT; Sigma-Aldrich) was administered IP (4 ng/g body weight) into chimeric CD11c-DTR mice every other day for 2 weeks while on diet. Control chimeric mice were injected IP with PBS.

Metabolic evaluation

Body weights were measured weekly and body composition determined using a Minispec NMR analyzer (Bruker Optics). Glucose tolerance tests (GTT) and insulin tolerance tests (ITT) were performed after a 6-hour fast. For GTT, mice were injected IP with D-glucose

(0.7 g/kg). For ITT, mice were injected IP with human insulin (1 unit/kg). For both GTT and ITT, blood glucose concentrations (mg/dl) were measured 0, 15, 30, 45, 60, 90, and 120 min after injection. Serum insulin (Crystal Chem) and MCP-1 (R&D system) were measured by ELISA. Non-esterified fatty acids (NEFA) in serum samples were measured using serum/plasma free fatty acid detection kits (Zen Bio). Total triglycerides were extracted from frozen liver samples (200 mg) and measured by colorimetric enzyme assay.

Confocal Microscopy

After consent, human omental adipose tissue samples were collected intraoperatively from patients undergoing bariatric surgery at the University of Michigan. All human use protocols were approved by the University of Michigan Institutional Review Board. Immunofluorescence staining was performed as described (Martinez-Santibanez et al., 2014) using the following antibodies: anti-HLA-DR (clone LN3, eBioscience), anti-CD206 (clone 309210, R&D Systems), anti-Caveolin (clone 2297, BD), anti-CD4 (clone A161A1, Biolegend). Images were collected using an Olympus Fluoview 100 laser scanning confocal microscope.

Intravital Two-Photon Microscopy

The day before intravital microscopy, 2.5×10^6 CFSE-labeled OTII $CD4^+$ T cells were adoptively transferred IP into recipient CD11c-mCherry mice. BSA or OVA (100 μg/mouse) was administrated 2 hours before imaging. Mice were anesthetized with pentobarbital (60 mg/kg body weight). Gonadal adipose tissue was surgically exposed and positioned in custom-built heated stage for intravital microscopy. Two-Photon imaging was performed with Leica 5P MP confocal microscope (Leica Microsystems) equipped with 20× numerical aperture objective with excitation with a Mai-Tai Ti:Sapphire laser (Spectra Physics) tunned to 800 nm. Emitted fluorescence was collected using a two-channel non-descanned detector. Four four-dimensional analysis of cell trafficking, stacks of 20 section (z step = 1 μm) were acquired every 1 min to provide an imaging volume of up to 20 μm in depth. Sequences of image stacks were transformed into volume-rendered four-dimensional movies using Imaris software (Bitplane) and the spot analysis was used for semi-automated tracking of cell motility in three dimensions by using the parameters of autoregressive motion as an algorithm 8 μm spot diameter and 20 μm maximum distance. Imaris software (Bitplane) was used to calculate T cell velocity, T cell displacement, and CD11c cell-CD4 cells interactions.

Isolation of Adipose Tissue SVCs and Flow Cytometry Analysis

SVCs from adipose tissues were isolated as previously described (Cho et al., 2014). Cells were incubated in Fc Block for 10 min on ice and stained with indicated antibodies for 30 min at 4°C. Stained cells were washed twice in PBS and fixed in 0.1% PFA before analysis. For intracellular staining and BrDU, cells were stained as described before (Morris DL et al., 2013). Analysis performed on FACSCanto II Flow Cytometer or FACSAria III (BD Bioscciences) and analyzed with FlowJo software (Treestar).

Cell Culture

Bone marrow cells were isolated from mice by flushing of tibia and fibula and differentiated into bone marrow derived macrophages (BMDM) as described (Singer et al., 2013). Differentiation was confirmed by demonstrating F4/80 expression by flow cytometry. Cells were placed in 10% serum media for 24 hours prior to treatment with LPS (10ng/ML) for 6 hours.

Gene expression analysis

RNA from tissues and cells was extracted using RNeasy Midi Kits (Qiagen) and cDNA generated from 0.5-1.0 μg total RNA using High Capacity cDNA Reverse Transcription Kits (Applied Biosystems). Power SYBR Green PCR Master Mix (Applied Biosystems) and the StepOnePlus System (Applied Biosystems) were used for real-time quantitative PCR. Arbp expression was used as an internal control for data normalization. Samples were assayed in duplicate and relative expression was determined using the $2^{-\Delta\Delta CT}$ method.

Immunoblotting Analyses

Mice were fasted for 6 hours and stimulated with insulin (3 U/kg body weight) or PBS IP. Liver and eWAT extracts were prepared 5 min after stimulation by homogenization in lysis buffer containing 50 mM Tris (pH 7.5), 1% Nonidet P-40, 150 mM NaCl, 2 mM EGTA, 1 mM Na_3VO_4, 100 mM NaF, 10 mM $Na_4P_2O_7$, and protease inhibitors (Roche, IN). Proteins was separated by SDS-PAGE, immunoblotted with indicated antibodies, and visualized using the Odyssey infrared imaging system (Li-Cor Bioscience, Lincooln, NE). Phospho-AKT (Ser473) and AKT antibody were purchased from Cell Signaling Technology.

Statistical Analysis

All values are reported as mean ± SEM. Differences between groups were determined using unpaired, two-tailed student t test or one-way ANOVA with Tukey post hoc tests using GraphPad Prism 5 software. P values less than 0.05 were considered significant.

Supplementary Material

Refer to Web version on PubMed Central for supplementary material.

Acknowledgments

This work was carried out with support from the NIH/NIDDK (DK090262 and DK092873 to C.N.L., DK095050 and DK097449 to R.W.O.) and the American Diabetes Association (07-12-CD-08). Trainees were supported by NIH NIAID Experimental Training in Immunology T32 AI007413-19 (B.Z), NIH NIDDK F32 DK091976 (D.L.M.), and an NIH Minority Training Supplement (DK090262-S1 to G.M-S.). This work utilized Core Services from the Michigan Nutrition and Obesity Research Center supported by grant DK089503 of NIH to the University of Michigan. This work utilized the Microscopy Core of the Michigan Diabetes Research Center funded by NIH 2P30-DK20572 from the National Institute of Diabetes & Digestive & Kidney Diseases.

References

Bertola A, Ciucci T, Rousseau D, Bourlier V, Duffaut C, Bonnafous S, Blin-Wakkach C, Anty R, Iannelli A, Gugenheim J, et al. Identification of adipose tissue dendritic cells correlated with

obesity-associated insulin-resistance and inducing Th17 responses in mice and patients. Diabetes. 2012; 61:2238–2247. [PubMed: 22596049]

Cho KW, Morris DL, Lumeng CN. Flow cytometry analyses of adipose tissue macrophages. Methods Enzymol. 2014; 537:297–314. [PubMed: 24480353]

Cipolletta D, Feuerer M, Li A, Kamei N, Lee J, Shoelson SE, Benoist C, Mathis D. PPAR-gamma is a major driver of the accumulation and phenotype of adipose tissue Treg cells. Nature. 2012; 486:549–553. [PubMed: 22722857]

Deiuliis J, Shah Z, Shah N, Needleman B, Mikami D, Narula V, Perry K, Hazey J, Kampfrath T, Kollengode M, et al. Visceral adipose inflammation in obesity is associated with critical alterations in tregulatory cell numbers. PLoS One. 2011; 6:e16376. [PubMed: 21298111]

Deng T, Lyon CJ, Minze LJ, Lin J, Zou J, Liu JZ, Ren Y, Yin Z, Hamilton DJ, Reardon PR, et al. Class II major histocompatibility complex plays an essential role in obesity-induced adipose inflammation. Cell Metab. 2013; 17:411–422. [PubMed: 23473035]

Do JS, Valujskikh A, Vignali DA, Fairchild RL, Min B. Unexpected role for MHC II-peptide complexes in shaping CD8 T-cell expansion and differentiation in vivo. Proc Natl Acad Sci U S A. 2012; 109:12698–12703. [PubMed: 22802622]

Fabbrini E, Cella M, McCartney SA, Fuchs A, Abumrad NA, Pietka TA, Chen Z, Finck BN, Han DH, Magkos F, et al. Association between specific adipose tissue CD4+ T-cell populations and insulin resistance in obese individuals. Gastroenterology. 2013; 145:366–374. e361–363. [PubMed: 23597726]

Feuerer M, Herrero L, Cipolletta D, Naaz A, Wong J, Nayer A, Lee J, Goldfine AB, Benoist C, Shoelson S, et al. Lean, but not obese, fat is enriched for a unique population of regulatory T cells that affect metabolic parameters. Nat Med. 2009; 15:930–939. [PubMed: 19633656]

Gautier EL, Shay T, Miller J, Greter M, Jakubzick C, Ivanov S, Helft J, Chow A, Elpek KG, Gordonov S, et al. Gene-expression profiles and transcriptional regulatory pathways that underlie the identity and diversity of mouse tissue macrophages. Nat Immunol. 2012; 13:1118–1128. [PubMed: 23023392]

Halin C, Rodrigo Mora J, Sumen C, von Andrian UH. In vivo imaging of lymphocyte trafficking. Annu Rev Cell Dev Biol. 2005; 21:581–603. [PubMed: 16212508]

Jung MY, Kim HS, Hong HJ, Youn BS, Kim TS. Adiponectin induces dendritic cell activation via PLCgamma/JNK/NF-kappaB pathways, leading to Th1 and Th17 polarization. J Immunol. 2012; 188:2592–2601. [PubMed: 22345647]

Khan IM, Dai Perrard XY, Perrard JL, Mansoori A, Wayne Smith C, Wu H, Ballantyne CM. Attenuated adipose tissue and skeletal muscle inflammation in obese mice with combined CD4+ and CD8+ T cell deficiency. Atherosclerosis. 2014; 233:419–428. [PubMed: 24530773]

Khanna KM, Blair DA, Vella AT, McSorley SJ, Datta SK, Lefrancois L. T cell and APC dynamics in situ control the outcome of vaccination. J Immunol. 2010; 185:239–252. [PubMed: 20530268]

Koltsova EK, Garcia Z, Chodaczek G, Landau M, McArdle S, Scott SR, von Vietinghoff S, Galkina E, Miller YI, Acton ST, et al. Dynamic T cell-APC interactions sustain chronic inflammation in atherosclerosis. J Clin Invest. 2012; 122:3114–3126. [PubMed: 22886300]

Lumeng CN, Bodzin JL, Saltiel AR. Obesity induces a phenotypic switch in adipose tissue macrophage polarization. J Clin Invest. 2007; 117:175–184. [PubMed: 17200717]

Marguerat S, MacDonald HR, Kraehenbuhl JP, van Meerwijk JP. Protection from radiation-induced colitis requires MHC class II antigen expression by cells of hemopoietic origin. J Immunol. 1999; 163:4033–4040. [PubMed: 10491007]

Martinez-Santibanez G, Cho KW, Lumeng CN. Imaging white adipose tissue with confocal microscopy. Methods Enzymol. 2014; 537:17–30. [PubMed: 24480339]

Mathis D. Immunological goings-on in visceral adipose tissue. Cell Metab. 2013; 17:851–859. [PubMed: 23747244]

Mattioli B, Straface E, Quaranta MG, Giordani L, Viora M. Leptin promotes differentiation and survival of human dendritic cells and licenses them for Th1 priming. J Immunol. 2005; 174:6820–6828. [PubMed: 15905523]

Moraes-Vieira PM, Yore MM, Dwyer PM, Syed I, Aryal P, Kahn BB. RBP4 Activates Antigen-Presenting Cells, Leading to Adipose Tissue Inflammation and Systemic Insulin Resistance. Cell Metab. 2014; 19:512–526. [PubMed: 24606904]

Morris DL, Cho KW, Delproposto JL, Oatmen KE, Geletka LM, Martinez-Santibanez G, Singer K, Lumeng CN. Adipose Tissue Macrophages Function as Antigen Presenting Cells and Regulate Adipose Tissue CD4+ T Cells in Mice. Diabetes. 2013; 62:2762–2772. [PubMed: 23493569]

Nishimura S, Manabe I, Nagasaki M, Eto K, Yamashita H, Ohsugi M, Otsu M, Hara K, Ueki K, Sugiura S, et al. CD8+ effector T cells contribute to macrophage recruitment and adipose tissue inflammation in obesity. Nat Med. 2009; 15:914–920. [PubMed: 19633658]

O'Rourke RW, White AE, Metcalf MD, Winters BR, Diggs BS, Zhu X, Marks DL. Systemic inflammation and insulin sensitivity in obese IFN-gamma knockout mice. Metabolism. 2012; 61:1152–1161. [PubMed: 22386937]

Odegaard JI, Chawla A. Alternative macrophage activation and metabolism. Annu Rev Pathol. 2011; 6:275–297. [PubMed: 21034223]

Patsouris D, Li PP, Thapar D, Chapman J, Olefsky JM, Neels JG. Ablation of CD11c-positive cells normalizes insulin sensitivity in obese insulin resistant animals. Cell Metab. 2008; 8:301–309. [PubMed: 18840360]

Podojil JR, Miller SD. Molecular mechanisms of T-cell receptor and costimulatory molecule ligation/blockade in autoimmune disease therapy. Immunol Rev. 2009; 229:337–355. [PubMed: 19426232]

Priceman SJ, Kujawski M, Shen S, Cherryholmes GA, Lee H, Zhang C, Kruper L, Mortimer J, Jove R, Riggs AD, et al. Regulation of adipose tissue T cell subsets by Stat3 is crucial for diet-induced obesity and insulin resistance. Proc Natl Acad Sci U S A. 2013; 110:13079–13084. [PubMed: 23878227]

Rangel-Moreno J, Moyron-Quiroz JE, Carragher DM, Kusser K, Hartson L, Moquin A, Randall TD. Omental milky spots develop in the absence of lymphoid tissue-inducer cells and support B and T cell responses to peritoneal antigens. Immunity. 2009; 30:731–743. [PubMed: 19427241]

Reis e Sousa C. Dendritic cells in a mature age. Nat Rev Immunol. 2006; 6:476–483. [PubMed: 16691244]

Rocha VZ, Folco EJ, Sukhova G, Shimizu K, Gotsman I, Vernon AH, Libby P. Interferon-gamma, a Th1 cytokine, regulates fat inflammation: a role for adaptive immunity in obesity. Circ Res. 2008; 103:467–476. [PubMed: 18658050]

Singer K, Morris DL, Oatmen KE, Wang T, DelProposto J, Mergian T, Cho KW, Lumeng CN. Neuropeptide Y is produced by adipose tissue macrophages and regulates obesity-induced inflammation. PLoS One. 2013; 8:e57929. [PubMed: 23472120]

Stefanovic-Racic M, Yang X, Turner MS, Mantell BS, Stolz DB, Sumpter TL, Sipula IJ, Dedousis N, Scott DK, Morel PA, et al. Dendritic Cells Promote Macrophage Infiltration and Comprise a Substantial Proportion of Obesity-Associated Increases in CD11c+ Cells in Adipose Tissue and Liver. Diabetes. 2012; 61:2330–2339. [PubMed: 22851575]

Stolarczyk E, Vong CT, Perucha E, Jackson I, Cawthorne MA, Wargent ET, Powell N, Canavan JB, Lord GM, Howard JK. Improved insulin sensitivity despite increased visceral adiposity in mice deficient for the immune cell transcription factor T-bet. Cell Metab. 2013; 17:520–533. [PubMed: 23562076]

Surh CD, Sprent J. Homeostasis of naive and memory T cells. Immunity. 2008; 29:848–862. [PubMed: 19100699]

Vandanmagsar B, Youm YH, Ravussin A, Galgani JE, Stadler K, Mynatt RL, Ravussin E, Stephens JM, Dixit VD. The NLRP3 inflammasome instigates obesity-induced inflammation and insulin resistance. Nat Med. 2011; 17:179–188. [PubMed: 21217695]

Winer S, Chan Y, Paltser G, Truong D, Tsui H, Bahrami J, Dorfman R, Wang Y, Zielenski J, Mastronardi F, et al. Normalization of Obesity-Associated Insulin Resistance through Immunotherapy: CD4+ T Cells Control Glucose Homeostasis. Nat Med. 2009; 15:921–929. [PubMed: 19633657]

Yang H, Youm YH, Vandanmagsar B, Ravussin A, Gimble JM, Greenway F, Stephens JM, Mynatt RL, Dixit VD. Obesity increases the production of proinflammatory mediators from adipose tissue

T cells and compromises TCR repertoire diversity: implications for systemic inflammation and insulin resistance. J Immunol. 2010; 185:1836–1845. [PubMed: 20581149]

Zhong J, Rao X, Braunstein Z, Taylor A, Narula V, Hazey J, Mikami D, Needleman B, Rutsky J, Sun Q, et al. T-cell costimulation protects obesity-induced adipose inflammation and insulin resistance. Diabetes. 2014; 63:1289–1302. [PubMed: 24222350]

Zhu J, Paul WE. CD4 T cells: fates, functions, and faults. Blood. 2008; 112:1557–1569. [PubMed: 18725574]

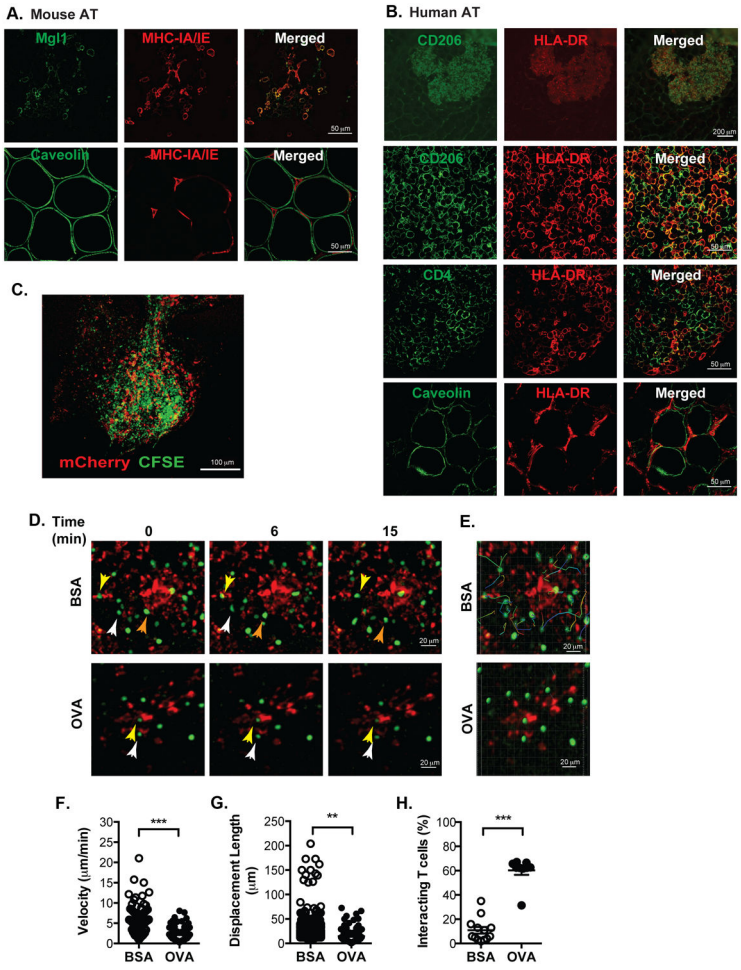

Figure 1. Adipose tissue macrophages (ATMs) physically interact with CD4$^+$ T cells in an antigen-dependent manner

(A) Immunofluorescence analysis of MHCII$^+$ cells (red) in FALCs (Fat-Associated Lymphoid Clusters) regions of mouse adipose tissue.

(B) Immunofluorescence analysis of HLA-DR$^+$ (red) cells in human omental tissue. Representative images presented from similar results from 5 independent samples.

(C) Maximum intensity projection of *z*-stacks in FALCs in eWAT from CD11c-mCherry mice adoptively transferred with CFSE-CD4$^+$ cells.

(D) Time-lapse images of interacting CD11c$^+$ ATMs (red) and OTII CD4$^+$ T cells (green) in eWAT from CD11c-mCherry mice injected with BSA (upper) or OVA (lower). Imaging of adipose tissue performed with intravital multi-photon confocal microscopy over a 20 minute imaging window.

(E) CD4$^+$ T cell migration pathways in adipose tissue from mice injected with BSA (upper) or OVA (lower).

(F) Velocity and (G) displacement lengths of individual CD4+ T cells in eWAT.

(H) Percent of CD4+ T cells interacting with CD11c+ cells in eWAT. Microscopy data are representative of three independent experiments.

Data are means ± SEM. ** $p < 0.01$, *** $p < 0.001$ versus BSA.

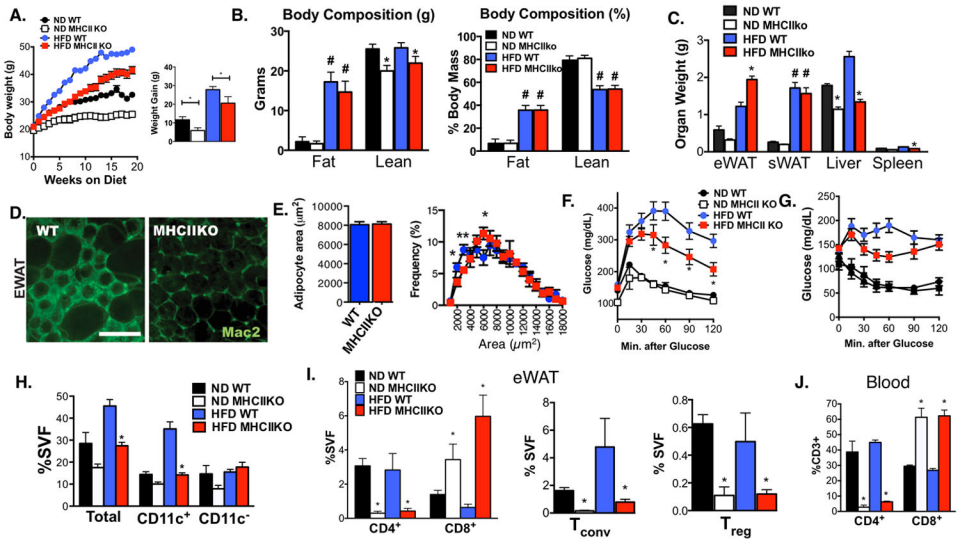

Figure 2. MHCII deficient mice are protected from HFD-induced insulin resistance through the reduction of ATMs and CD4$^+$ ATT accumulation

MHCIIKO (KO) and WT control male mice were fed ND or HFD for 20 weeks. (A) Body weights of WT and MHCIIKO (KO) mice during ND and HFD feeding (ND: $n = 6$; HFD: $n = 8$).

(B) Body composition analysis of fat and lean mass in WT and KO mice as determined by NMR. Right panel shows normalization to total body weight.

(C) Organ weights at the end of the diet exposure.

(D) Immunofluorescence identification of Mac2$^+$ ATMs in eWAT from HFD fed WT and KO mice. Scale bar = 200 μm.

(E) Adipocyte size and adipocyte size distribution in eWAT from HFD fed WT and KO mice.

Analysis of glucose metabolism by (F) GTT and (G) ITT.

(H) Quantitation of Total, CD11c$^+$, and CD11c$^-$ ATMs (CD11 b$^+$F480$^+$) in eWAT from WT and KO mice by flow cytometry.

(I) Quantitation of CD3$^+$ CD4$^+$ and CD3$^+$ CD8$^+$ ATTs (left), Tconv and Treg (right) in eWAT in WT and KO mice.

(J) Quantitation of blood CD3$^+$ CD4$^+$ and CD3$^+$ CD8$^+$ T lymphocytes from WT and KO mice.

Data are shown as means ± SEM. # $p<0.05$ in one-way ANOVA, * $p<0.05$, ** $p<0.01$, *** $p<0.001$ versus WT.

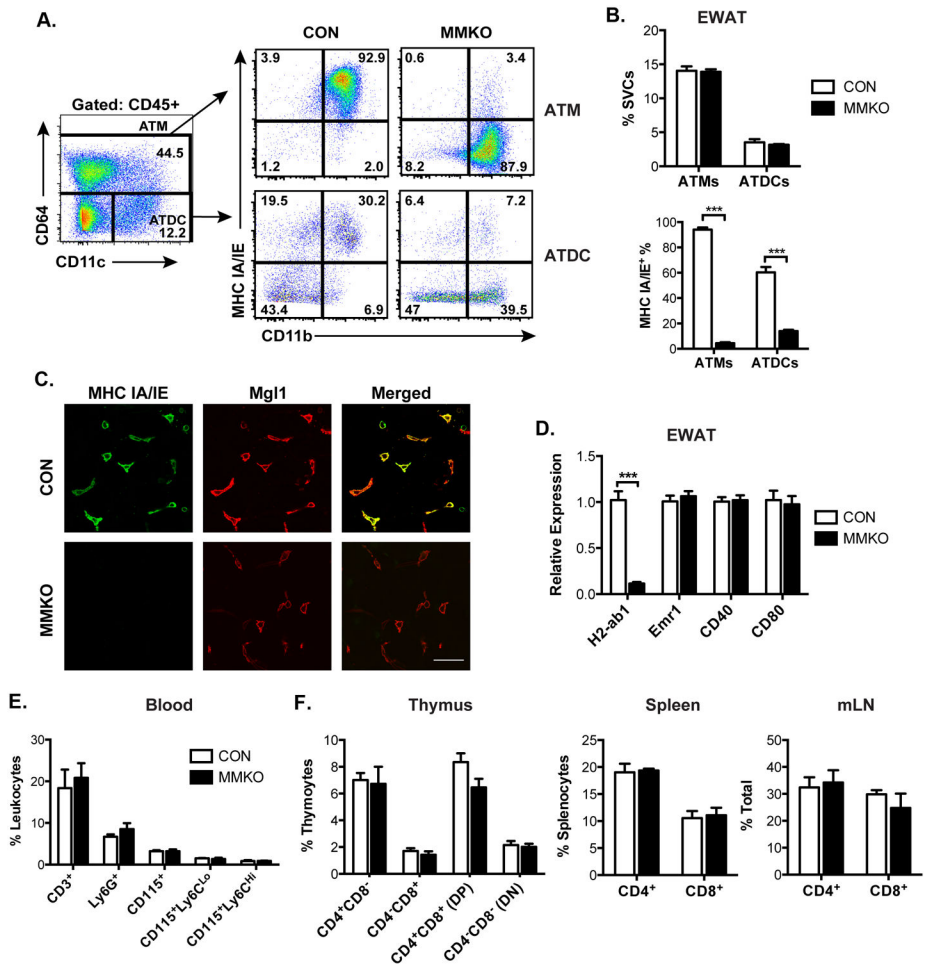

Figure 3. Generation of macrophage-specific MHCII knockout (MMKO) mice

(A) Representative flow cytometry plots of MHCII-expressing cells in eWAT SVCs. ATMs ($CD45^+$ $CD64^+$) (upper panels) and ATDCs ($CD45^+$ $CD64^-$ $CD11c^+$) (lower) from control (CON) and MMKO mice.

(B) Quantitation of ATMs and ATDCs (upper) and frequency of $MHCII^+$ cells in ATMs and ATDCs (lower) from CON and MMKO mice. 5 mice assessed per group in 4 independent cohorts.

(C) Immunofluorescence images showing loss of $MHCII^+$ expression in (green) and resident $Mgl1^+$ ATMs (red). Scale bar = 50 μm.

(D) qPCR analysis of eWAT from CON and MMKO mice

(E) Quantitation of total blood myeloid cells and total lymphocytes.

(F) Frequency of $CD4^+$ and $CD8^+$ T lymphocytes in thymus, spleen and mesenteric lymph nodes (mLN).

Data are means ± SEM. ***, p <0.001 vs. CON.

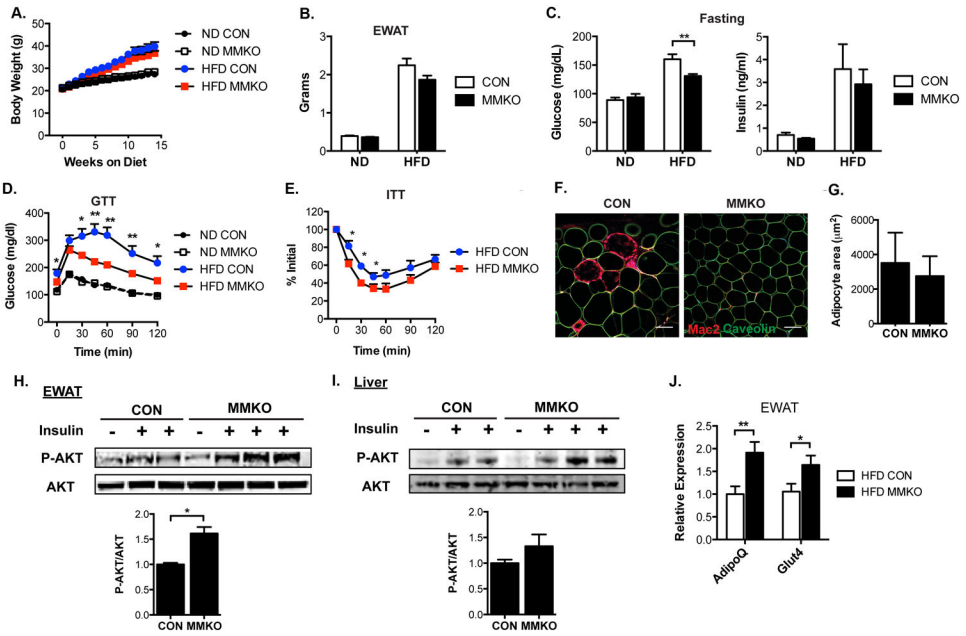

Figure. 4. Macrophage-specific MHCII knockout mice have attenuated HFD-induced insulin resistance due to improved adipose tissue insulin sensitivity

Metabolic assessment of MMKO and control mice fed ND or HFD for 14 weeks (*n*=10-12 for each group).

(A) Body weight.

(B) eWAT weight.

(C) Fasting glucose (left) and insulin levels (right).

(D) GTT and (E) ITT performed at 12 weeks of diet exposure.

(F) Immunofluorescence image of $Mac2^{+}$ ATM (red) and $caveolin^{+}$ adipocytes (green) in eWAT from HFD fed CON and MMKO mice. Scale bar = 100 μm.

(G) Quantitation of adipocyte size in eWAT from HFD-fed CON and MMKO.

12 weeks after HFD feeding, tissues were harvested from CON and MMKO mice 5 min after intravenous injection of saline or insulin.

(H-I) Immunoblots of lysates from eWAT (H) and liver (I) with anti-pSer473 or anti-Akt (upper) and quantitation of phosphorylated AKT normalized to total AKT levels (lower).

(J) Gene expression in eWAT from HFD fed CON and MMKO.

Data are means ± SEM. * p <0.05, ** p<0.01 versus CON.

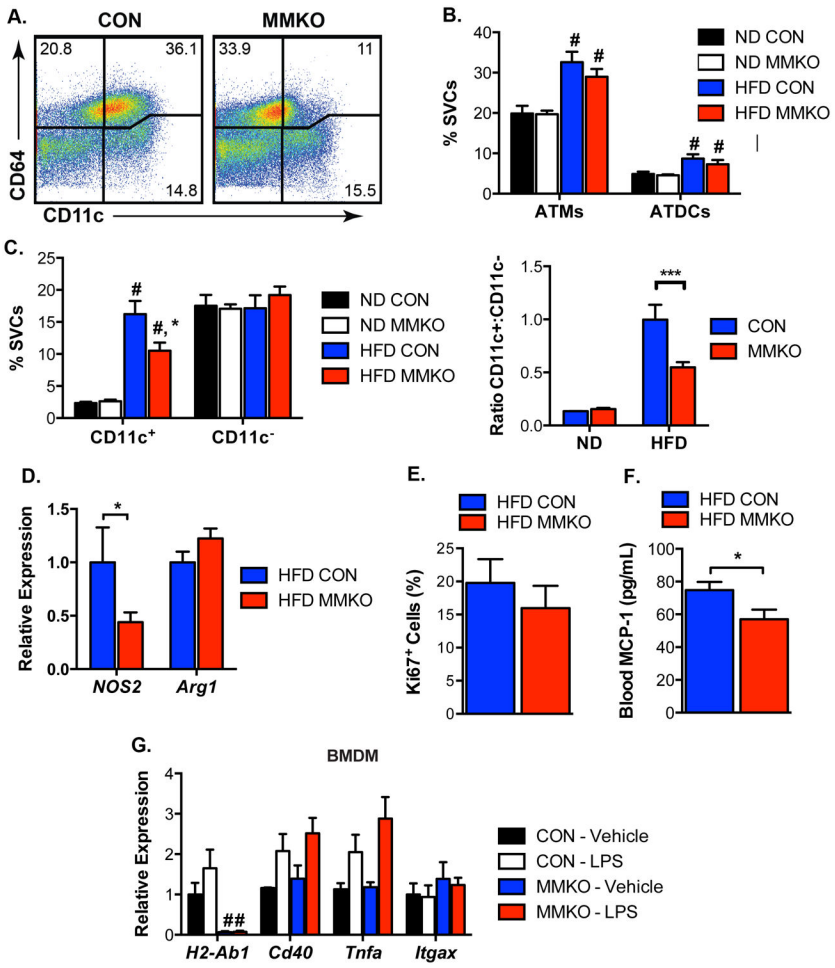

Figure 5. Macrophage-specific MHCII deficiency reduced HFD-induced CD11c+ ATMs accumulation in visceral fat

(A) Representative flow cytometry plots of $CD45^+$ cells in SVC from eWAT from HFD-fed CON and MMKO. ATMs ($CD45^+$ $CD64^+$) are differentiated based on CD11c expression. ATDCs are defined as $CD64^-$ $CD11c^+$.

(B) Quantitation of ATM and ATDC content in eWAT.

(C) Frequency of $CD11c^+$ ATMs and $CD11c^-$ ATMs (left) and the ratio of $CD11c^+$ ATMs to $CD11c^-$ ATMs (right) in eWAT.

(D) Gene expression in eWAT from HFD fed CON and MMKO.

(E) Quantitation of Ki67+ cells frequency in eWAT from HFD fed CON and MMKO.

(F) Blood CCL2 (MCP-1) concentration from HFD-fed CON and MMKO.

(G) Gene expression in bone marrow-derived macrophages (BMDM) from CON and MMKO in the absence or presence of 10 ng/ml LPS for 6 hours.

Data are means ± SEM. # p <0.05 in groups, * p <0.05, *** p<0.001 versus CON.

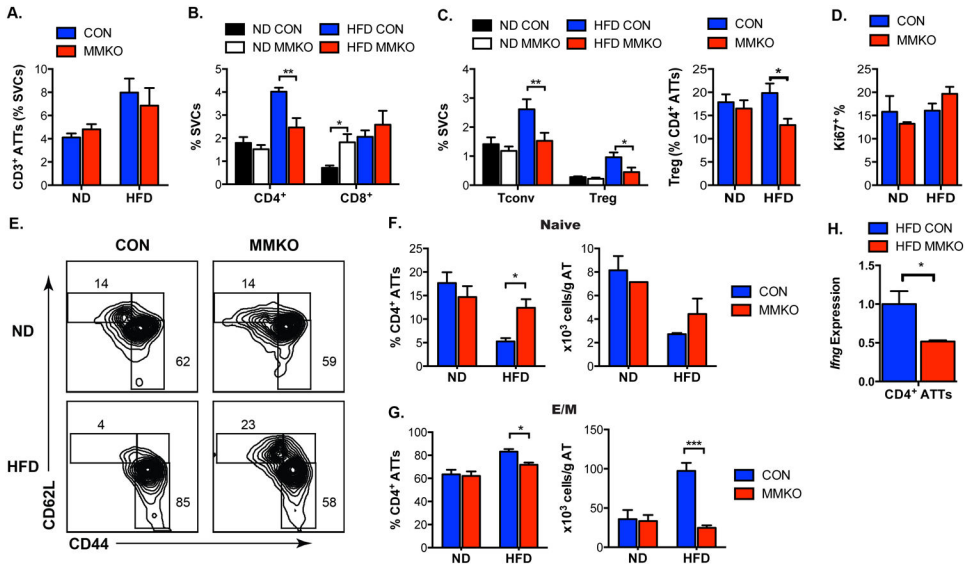

Figure 6. Macrophage-specific MHCII deficiency reduces obesity-induced CD4$^+$ ATT accumulation and maturation

Quantitation of (A) CD3$^+$ ATTs and (B) CD4$^+$ and CD8$^+$ ATTs in eWAT.

(C) Quantitation of Tconvs and Tregs in eWAT expressed as % SVCs (left) and as % CD4$^+$ ATTs (right) in CON and MMKO.

(D) Frequency of proliferating Ki67$^+$ CD4$^+$ ATTs in eWAT.

(E) Representative flow cytometry plots gated on CD3$^+$ CD4$^+$ cells to quantify effector-memory (E/M; CD44^{high} CD62L$^-$), central-memory (C/M; CD44^{high} CD62L$^+$) and naïve (CD44^{low} CD62L$^+$) CD4$^+$ ATT subsets in eWAT.

(F) Quantitation of naïve CD4$^+$ ATT subsets in eWAT.

(G) Quantitation of E/M CD4$^+$ ATT subsets in eWAT.

(H) *Ifng* gene expression in FACS-sorted CD4$^+$ ATTs from HFD-fed CON and MMKO.

Data are means ± SEM. * p <0.05, ** p <0.01, *** p<0.001 versus CON.

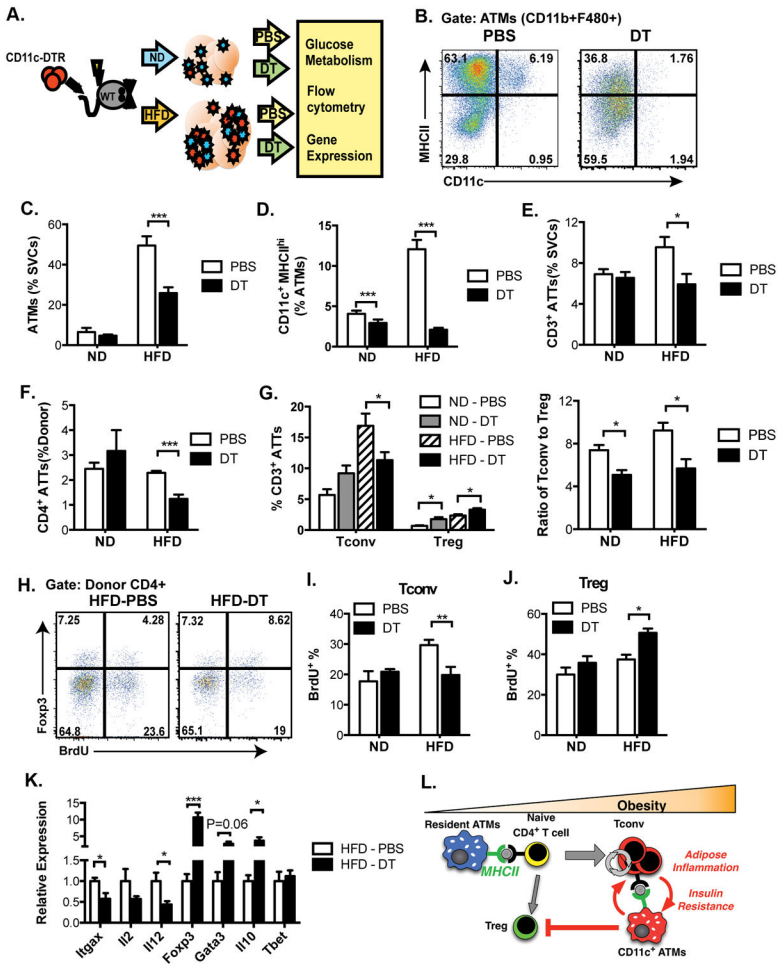

Figure 7. Ablation of CD11c decreases CD4$^+$ ATT accumulation and proliferation in response to obesity

(A) Schematic diagram of experimental design of diphtheria toxin (DT)-mediated ablation of CD11c expressing cells. 5 mice per group were analyzed.

(B) Representative analysis of MHCII expression in ATMs (CD11b$^+$F480$^+$) in eWAT from PBS or DT-treated HFD fed mice demonstrating loss of MHCII^{high} cells with DT.

Quantification of (C) ATMs, (D) CD11c$^+$MHCII^{HI} ATMs, (E) CD3$^+$ ATTs, and (F) CD4$^+$ ATTs in eWAT.

(G) Quantification of Tconv and Treg (left) and the ratio of Tconv to Treg (right) in eWAT.

(H) Representative analysis of CD4$^+$ ATTs after BrdU injection to identify proliferating cells. Cells gated on CD3$^+$ CD4$^+$ ATTs and then examined for FoxP3 and BrdU intracellular staining to assess Tconv (Foxp3$^-$) and Treg (Foxp3$^+$) ATT in HFD fed mice.

Quantitation of proliferating (I) Tconv and (J) Treg in eWAT

(K) qRT-PCR analysis of eWAT from PBS or DT-treated HFD mice.

Data are means ± SEM. * p <0.05, ** p <0.01, *** p <0.001 versus PBS.

(L) Graphical Model.